

INVESTIGATING THE DARK MATTER DISTRIBUTION WITH NGST

Peter Schneider¹ and Jean-Paul Kneib²

¹Max-Planck-Institut für Astrophysik, Postfach 1523, D-85740 Garching, Germany

²Observatoire Midi-Pyrénées, 14 Av. E. Belin, F-31400 Toulouse, France

ABSTRACT

The developments summarized with the name “weak gravitational lensing” have led to exciting possibilities to study the (statistical properties of the) dark matter distribution in the Universe. Concentrating on those aspects which require deep wide-field imaging surveys, we describe the basic principles of weak lensing and discuss its future applications in view of NGST (a) to determine the statistical properties of the dark matter halos of individual galaxies, (b) to determine the mass and the mass profile of very low-mass clusters and groups at medium redshift and/or of more massive clusters at very high redshift, and (c) to measure the power spectrum of the matter distribution in the Universe in the non-linear regime, thereby also obtaining a mass-selected sample of halos and providing a means to investigate the scale- and redshift dependence of the bias ‘factor’.

1. INTRODUCTION

Ultra-deep observations with NGST will reveal the distribution and the physical properties of very high-redshift galaxies. Precursors of our present-day galaxies can be studied with unprecedented accuracy, exploring regions of parameter space (redshift, luminosity, size) which are currently white spots on our ‘map of knowledge’. The remaining link between these new insights into the evolution of galaxies and structure formation and cosmology is the relation between optical/IR properties of galaxies and their precursors and the mass of the halo in which they are embedded. Bridging this gap between the luminous properties of matter concentrations and modelling of the formation of structure is essential for our understanding of the evolution of galaxies, groups, and clusters, and that of the Universe as a whole.

Gravitational lensing is probably the only method which can provide this missing link. Probing the tidal gravitational field of mass concentrations (or, more generally, of the intervening mass distribution) by the distortion of light bundles originating from background galaxies, the mass of galaxies, groups, and clusters can be determined individually, or statistically. The unique feature of gravitational lensing is that the total matter distribution is probed, independent of the physical nature or state of the matter, and independent of symmetry assumptions.

The weak gravitational lensing effect has been studied in

great detail recently, and applied successfully to several (classes of) systems; in particular, the projected (dark) matter distribution of several relatively low-redshift clusters of galaxies has been reconstructed, using both parametric and parameter-free approaches, (e.g., Fahlman et al. 1994; Smail et al. 1995; Squires et al. 1996a,b; Seitz et al. 1996, 1998; Luppino & Kaiser 1997a; Hoekstra et al. 1998), and the mass and physical scale of galaxy halos has been constrained statistically, employing the so-called galaxy-galaxy lensing effect (Brainerd et al. 1996; Griffiths et al. 1997; Hudson et al. 1998). Furthermore, clusters of galaxies have been detected from observing their tidal gravitational field through the image distortion of faint background galaxies (e.g., Luppino & Kaiser 1997b), thus allowing to define a sample of clusters from their mass properties only, i.e., without referring to their luminous properties (Schneider 1996).

Before continuing describing scientific applications of weak lensing, we shall first outline the basic method.

2. TIDAL DISTORTION OF GALAXY IMAGES

A gravitational lens provides a map from the observer’s sky to the undistorted sky, caused by the gravitational field of the deflector. The deflection angle is determined by the mass distribution of the lens, and the mapping from the source to the observable images depends in addition on the redshifts of the sources and the lens. Light bundles are not only deflected as a whole, but due to the tidal component of the gravitational potential, they are distorted. The image of a circular source will, to first order, be an ellipse. Thus, if all background galaxies were circular, the observable ellipticity of galaxy images would provide a direct means to measure the local tidal gravitational field of the lens. Since galaxies are intrinsically not circular, this simple method is impractical. However, since it can be assumed that the orientation of galaxies is random, a tidal field would cause a preferred orientation of the images, or, if ellipticity is considered as a two-dimensional quantity, it would cause a net ellipticity. The distortions are such that galaxy images are preferentially aligned tangent to the ‘mass center’, such as is clearly visible for the giant luminous arcs.

Denote by $\epsilon^{(s)}$ the complex intrinsic ellipticity of a galaxy (defined in terms of its second order brightness moments), and let ϵ be the corresponding complex ellipticity of the observed image. The variable ϵ is defined such that for an image with elliptical isophotes of axis ratio r and orientation φ of the major axis relative to a fixed reference

direction, $\epsilon = (1 - r)/(1 + r)e^{2i\varphi}$. The locally linearized gravitational lens equation yields the transformation between $\epsilon^{(s)}$ and ϵ , which for the case of weak distortions reads

$$\epsilon = \epsilon^{(s)} + \gamma, \quad (1)$$

and γ is the shear or the tidal gravitational field of the lens (for definition, see, e.g., Schneider, Ehlers & Falco 1992) defined in terms of the trace-free part of the Hessian of the gravitational potential. The random orientation of intrinsic ellipticities then implies that the expectation value of ϵ equals γ , and the noise of this estimator is determined by the width of the intrinsic ellipticity distribution: to measure a shear with precision $\Delta\gamma$, one needs $N \sim \sigma_\epsilon^2/(\Delta\gamma)^2$ galaxy images. Therefore, in order to measure a weak shear signal, N must be large, which can be achieved by either increasing a local ‘smoothing scale’ – thereby erasing small-scale structure information, or by increasing the number density of galaxy images, that is, by taking very deep images.

In the past few years, observational progress was made possible by the development of optical imaging instruments with extremely good image quality and/or wide-angle capability. These instruments made it possible to obtain images of thousands of faint galaxies (where faint means $I \sim 24.5$, where the number density of galaxies is about 30 per square arcminute). Weak lensing observations with 8-meter class telescopes will allow to obtain even deeper images; recent cluster mass reconstructions obtained from Keck images used a number density of about 60 galaxies/(arcmin)² (Clowe et al. 1998). However, longer exposures do not guarantee a higher number density of useful galaxy images, as fainter objects tend to become smaller: galaxies much smaller than the extent of the seeing disk do not carry much shape information and can therefore not be used. Seeing circularizes images, and sophisticated methods to correct for this effect have been developed (Bonnet & Mellier 1995; Kaiser et al 1995; van Waerbeke et al 1997). However, the factor by which the measured ellipticity must be multiplied to get the true (before seeing) ellipticity also multiplies the error of the measurement – the smaller the galaxy relative to the size of the seeing disk, the more uncertain becomes the determination of the ‘true’ ellipticity.

3. WEAK LENSING WITH NGST

Let us consider the specific example of a singular isothermal sphere with l.o.s. velocity dispersion σ_v . For this specific mass profile, an optimal statistics for the *detection* of this halo can be defined,

$$X \propto \sum_i \frac{\epsilon_{ti}}{\theta_i}, \quad (1)$$

where θ_i is the separation of a background galaxy relative to the center of the lens, and ϵ_{ti} is the tangential component of the image ellipticity (see, e.g., Schneider 1996). The sum extends over all background galaxies within an annulus $\theta_1 \leq \theta \leq \theta_2$, where the inner radius is constrained by the ability to measure ellipticities reliably for images very close to the foreground galaxy (or, in the case of clusters, where the isothermal assumption breaks down due to flattening of the mass profile near the center), and the outer radius is determined either by considering neighboring foreground galaxies, or the decline of the mass profile

relative to an isothermal profile. The signal-to-noise ratio of this statistics can be calculated to be

$$\begin{aligned} \frac{S}{N} &= 12.7 \left(\frac{n}{30 \text{arcmin}^{-2}} \right)^{1/2} \left(\frac{\sigma_\epsilon}{0.2} \right)^{-1} \\ &\times \left(\frac{\sigma_v}{600 \text{km/s}} \right)^2 \left(\frac{\ln(\theta_2/\theta_1)}{\ln(10)} \right)^{1/2} \left\langle \frac{D_{ds}}{D_s} \right\rangle, \end{aligned} \quad (2)$$

where D_{ds} and D_s are the angular-diameter distances from the lens and the observer to the source, respectively; the angular bracket denotes an average over the source population (the ratio D_{ds}/D_s is set to zero for galaxies with smaller redshift than the lens), and σ_ϵ is the dispersion of the intrinsic ellipticity distribution. The larger S/N, the more details of the mass profile can be inferred from weak lensing observations.

The foregoing estimate allows us to discuss the unique features of NGST for weak lensing:

(1) Depth: the large aperture, combined with the largely reduced sky background, allows the imaging of much fainter galaxies than currently feasible. This will lead to a much larger number density n of galaxy images which can be used for these studies, and (most likely) to a considerably higher mean redshift of the galaxies, increasing the geometrical factor D_{ds}/D_s .

(2) Angular resolution: Since galaxies tend to become smaller with decreasing brightness, the number of galaxies that can be used for weak lensing studies depends on the angular resolution; only galaxies which are not significantly smaller than the size of the PSF can have a reliable shape measurement. The unique angular resolution of NGST will allow to measure the shapes of highest-redshift galaxies provided they are larger in extent than $\sim 500h^{-1}$ parsec, all of which contribute to n . Hence, even if the 10-meter class ground-based telescopes will carry out imaging surveys at significantly fainter magnitudes than currently available, their use for the weak lensing studies as outlined above will be limited, due to the small size of the very faint galaxies compared to the ground-based PSF. In addition, sampling of the PSF is essential for measuring accurate image ellipticities.

(3) Wavelength range: Since NGST provides images in the NIR with comparable or larger depth than even the HDF in the optical, it maps the visual-to-red emission of high-redshift galaxies which is expected to be considerably more regular than the rest-frame UV radiation. Since the noise of mass measurements increases proportionally to the dispersion σ_ϵ of the intrinsic ellipticities of the background galaxies, mass estimates obtained from typical NGST wavebands will be more accurate than from optical telescopes. In addition, wavelength coverage from the visual to 5μ will allow precise redshift estimates from multicolor photometry in which case the D_{ds}/D_s ratio no longer is a statistical quantity, but can be determined for each background galaxy separately, which will allow the use of more sensitive estimators than (1).

(4) Wide-angular field imaging: Nearly all applications of weak lensing depend on solid angle ω_{cam} covered per exposure: for a given science goal, the total observing time scales like ω_{cam}^{-1} . Compared to the WFC-part of the WFCP-2, the currently planned 8K camera provides a gain of a factor ~ 3.5 in ω_{cam} , and hardly any gain compared to the Advance Camera. However, *this is another one of the science cases where switching to a larger-size*

CCD mosaic would immediately reduce the observing time needed, or for given observing time, would enable more ambitious science goals to be obtained. E.g., switching to an 16K mosaic, such as soon will become routinely available for optical wavelength, would yield an advantage by a factor of 16 relative to the WFC.

Quantitative predictions of the quantities relevant for NGST images are highly model dependent and therefore uncertain. For example, current number counts in the K-band extend to about $K \sim 24$, whereas even a short exposure (20 minutes) with NGST will easily reach $K \sim 27$ (for a S/N per object of 5). Hence, one has to extrapolate at least 3 magnitudes into the dark. The limiting magnitude depends also on the (unknown) size of these faint galaxies; in a few hours of integration, $K = 29$ (S/N=5) can be reached if the size of galaxies is smaller than about 0.2 arcseconds. Roughly speaking, for a typical integration time of one hour, one can reach a limiting magnitude of about $K = 28$ for extended objects with sufficient S/N, probably yielding a number density of $\sim 2 \times 10^6 \text{ deg}^{-2}$, or a factor of ~ 20 larger than those which are currently used for weak lensing. In addition, the redshift distribution of these galaxies will extend to much higher redshifts, increasing the geometrical factor $D_{\text{ds}}/D_{\text{s}}$; this effect is particularly important for the high-redshift lenses. Generally speaking, this implies that *weak lensing studies can be extended with NGST to much less massive and/or higher redshift matter concentrations than currently possible.*

Next, three specific application shall be discussed in somewhat more detail.

4. DETERMINING THE STATISTICAL PROPERTIES OF THE DARK MATTER HALOS OF GALAXIES

Individual galaxy halos are not massive enough to be ‘seen’ with weak lensing, but the lensing effect of many foreground galaxies can be superposed.

The basic principle here is to study a statistical alignment of the images of background galaxies relative to their nearest neighboring foreground galaxies. Assuming for a moment that the redshifts of all galaxies are known, and that the massive properties of the galaxies (such as a velocity dispersion and a truncation scale length) scale with luminosity, the shear for each background galaxy can be predicted, and a likelihood function in terms of the mass parameters can be defined and maximized (Schneider & Rix 1997). If the redshifts are unknown, the likelihood function has to be averaged over the magnitude-dependent redshift probability distribution.

In a first application using ground-based data, Brainerd et al (1996) have shown that the rotational velocity of an L_* field galaxy is about 220 km/s, very much in accord with spectroscopically derived results, but measured for higher-redshift ($\langle z \rangle \sim 0.3$) galaxies. Further results using the Medium Deep Survey (Griffiths et al 1997) and the HDF (Dell’Antonio & Tyson 1996, Hudson et al 1998) have demonstrated the superiority of space-based imaging. In these studies, the number of galaxy-galaxy pairs was not sufficient to put upper bounds on the halo sizes of galaxies, but strict lower bounds have been obtained.

NGST will allow to greatly extend these studies, in

that the achievable depth and superior angular resolution and field-of-view will permit to study higher-redshift galaxy halos, less massive halos, and also avoid the use of excessive parametrization of the massive properties of galaxies, but by investigating the halos of galaxies with specific properties (such as photometric redshift estimates, magnitude, colors, morphology).

Assuming N_f ‘identical’ galaxy halos, the S/N for their detection is $\propto N_f^{1/2}$. To reach a given value of S/N, one needs

$$N_f = 350 \left(\frac{S/N}{10} \right)^2 \left(\frac{n}{600 \text{ arcmin}^{-2}} \right)^{-1} \left(\frac{\sigma_\epsilon}{0.2} \right)^2 \quad (3)$$

$$\times \left(\frac{\sigma_v}{150 \text{ km/s}} \right)^{-4} \left(\frac{\ln(\theta_2/\theta_1)}{\ln(10)} \right)^{-1} \left(\frac{\langle D_{\text{ds}}/D_{\text{s}} \rangle}{0.15} \right)^{-2}$$

of these foreground galaxies ($D_{\text{ds}}/D_{\text{s}} = 0.15$ in an EdS-Universe for $z_{\text{d}} = 3$ and $z_{\text{s}} = 5$). Note that a S/N of 10 means that σ_v of these galaxies can be determined with a 5% accuracy, or that additional parameters of the mass profile (such as a truncation radius) can be determined.

Investigating galaxies at $K \sim 24$ which will cover a broad redshift interval $1 \lesssim z \lesssim 5$ and which have a surface number density of $\sim 4 \times 10^5 \text{ mag}^{-1} \text{ deg}^{-2}$, and splitting these galaxies into bins of width $\Delta z = 0.1$ and $\Delta K = 0.1$ to define ‘similar galaxies’, we obtain about 10^3 galaxies per bin and per deg^{-2} . Of course, different binning is also possible, e.g., with larger Δz (related to the accuracy of photometric redshift estimates) and according to morphology or color. In any case, the assumption of about 400 bins is physically meaningful. Thus, for the assumed fiducial parameters, $\sim 0.35 \text{ deg}^2$ are needed to obtain a S/N of ten in a typical bin. As was pointed out by Schneider & Rix (1997), and observationally verified by Hudson et al. (1998) for the HDF, photometric redshifts will greatly increase the accuracy of the mass parameters of galaxy halos; this is likely to be even more relevant for high-redshift galaxies (where the redshift distributions of galaxies with vastly different magnitudes will strongly overlap).

Galaxy-galaxy lensing will allow to study the evolution of halo masses and size with redshift (at fixed luminosity), color, and morphology, the verification and cosmological evolution of Tully-Fischer-like scaling relations, and their dependence on environment (e.g., field galaxies versus galaxies in pairs versus cluster/group galaxies – see Natarajan & Kneib 1997; Geiger & Schneider 1998a; Natarajan et al. 1998), using maximum-likelihood techniques (Schneider & Rix 1997; Geiger & Schneider 1998b). Whereas preliminary studies of galaxy-galaxy lensing in clusters may indicate that the halo size of galaxies in clusters is smaller than that for field galaxies, these studies suffer from the very limited statistics currently available. Cluster observations with the ACS will improve the observational situation substantially, at least for medium-redshift clusters, but the full power of this method can only be exploited by the depth of NGST images which will allow an extension to high-redshift clusters.

In addition to weak lensing, given the depth of images routinely obtained with NGST, these exposures will contain typically several strong lensing systems, where a high-redshift faint galaxy will be mapped into two or more images by a foreground galaxy, thus allowing an accurate estimate of the mass of the latter. Note that several

such candidate multiple image systems have been found in the HDF (Hogg et al. 1996). The probability of a given source at high redshift to be multiply imaged depends on the evolution of the halo abundance, but is typically a few $\times 10^{-4}$. With a number density of $\sim 600 \text{arcmin}^{-2}$, and a field of view of $\sim 16 \text{arcmin}^2$, observing multiply imaged galaxies in virtually every NGST image is certain. To identify them, the high angular resolution of NGST to find morphologically similar galaxy images will be of utmost importance, together with multi-color information. The same observations required for the weak lensing programs mentioned above will then be useful to constrain the halo abundance on mass scales down to a few $\times 10^9 M_\odot$ as a function of redshift.

By combining these results on halo masses with the optical/IR properties of galaxies, the missing link between dark matter models and galaxy observations can be provided.

5. DETERMINING THE MASSES OF HIGH-REDSHIFT CLUSTERS/GROUPS

The S/N estimate (2) shows that current ground-based weak lensing studies can detect clusters with $\sigma_v \gtrsim 600$ km/s, and determine the mass profile only for more massive clusters. Changing to the NGST, a factor of ~ 20 in the galaxy number density, plus the higher redshift of the background galaxies, will change the ‘threshold’ to $\sigma_v \sim 250$ km/s for low-redshift clusters ($z \sim 0.3$), and/or allow to study the mass profiles of much higher-redshift clusters.

In order for clusters to be useful cosmological probes, their mass properties need to be understood. Whereas current and future wide-field imaging surveys will yield a large number of high-redshift candidate clusters, the abundance of massive clusters needs to be investigated by measuring their mass. Note that at higher redshift, assumptions about dynamical and thermal equilibrium, or symmetry, are probably less justified than at low redshift, making lensing an essential tool for measuring the mass of high-redshift clusters. Writing the estimate (2) as appropriate for NGST, one finds

$$\frac{S}{N} = 7.1 \left(\frac{n}{600 \text{arcmin}^{-2}} \right)^{1/2} \left(\frac{\sigma_\epsilon}{0.2} \right)^{-1} \times \left(\frac{\sigma_v}{250 \text{km/s}} \right)^2 \left(\frac{\ln(\theta_2/\theta_1)}{\ln(10)} \right)^{1/2} \frac{\langle D_{ds}/D_s \rangle}{0.72}, \quad (4)$$

where the fiducial value for D_{ds}/D_s applies for $z_d = 0.4$, $z_s = 4$ in an EdS Universe, or

$$\frac{S}{N} = 6.1 \left(\frac{n}{600 \text{arcmin}^{-2}} \right)^{1/2} \left(\frac{\sigma_\epsilon}{0.2} \right)^{-1} \times \left(\frac{\sigma_v}{500 \text{km/s}} \right)^2 \left(\frac{\ln(\theta_2/\theta_1)}{\ln(10)} \right)^{1/2} \frac{\langle D_{ds}/D_s \rangle}{0.155}, \quad (5)$$

with the fiducial value of D_{ds}/D_s taken for $z_d = 3$, $z_s = 5$. Hence one sees that the NGST will be able to greatly extend the investigation of cluster masses and mass distributions into regions of the mass-redshift space where currently no reliable information on cluster masses is available. In particular, the cosmic evolution of the

morphology and the amount of substructure, and its relation to the galaxy distribution (Kaiser & Squires 1993, Seitz & Schneider 1995, 1996; Squires et al 1996a,b, 1997; Seitz et al 1996, 1998; Hoekstra et al 1998) can be studied at high redshift.

Different classes of cluster candidates can then be investigated: those obtained from matched-filter analyses of optical images (e.g., Postman et al. 1996; Olsen et al. 1998), surface brightness enhancement (Dalcanton et al. 1998), candidate clusters from SZ surveys, as will be obtained, e.g., by the PLANCK Surveyor, extended sources from future X-ray missions etc. The various search methods are likely to yield classes of clusters which differ in their mass properties. Also, particularly interesting cases can be studied, such as pairs of clusters, to search for connecting filaments, and one might observe directly projected mass distributions which characterize ongoing merging of cluster pairs.

With background sources at typical redshifts of $z_s \sim 5$, and a sensitivity to very low-mass dark matter halos, the Universe becomes ‘optically thick’ to dark halos. Hence, along a given line-of-sight to redshift 5, there will be more than one dark halo within a few arcminutes which can be probed by (and which will affect) weak lensing. Therefore, it is essential to ‘slice’ the lenses into redshift bins, or more practically, to use the sensitivity of the lensing strength to the redshift of lens and source, expressed by D_{ds}/D_s . This can be achieved by using redshift information about the background galaxies, i.e., though relatively accurate photometric redshifts. It should be noted that this argument can be turned around: the dependence of the lensing strength on the redshifts can be used to put constraints on the source redshift distribution (Bartelmann & Narayan 1995), and thus to test the accuracy of photometric redshifts. Not much theoretical work has yet been done on such redshift-dependent methods; future work, in combination with ray tracing through model Universes obtained from N-body simulations (e.g., Wambsganss et al. 1998; Jain et al. 1998) will clarify the power and limitations of these applications.

Deep imaging of relatively low-redshift clusters will also be extremely useful for strong-lensing applications. Given that a few-orbit exposure with the HST-WFPC-2 reveals about ten strong lensing candidate features (such as arclets; multiply-imaged galaxies) in a strong cluster (e.g., A370 – see Kneib et al. 1993; A2218, Kneib et al. 1995, 1996; MS1512, Seitz et al. 1998), it is clear that a moderately long exposure with NGST will probably detect of order one hundred such strong lensing features; and probably also more reliably than with WFPC-2, due to the better angular resolution which is needed to compare candidate multiple images by their morphology. We show in Fig. 1 a first hint of what an NGST image of the cluster A2218 might look like. Also here, multi-color images will be tremendously helpful. With these numerous strong lensing constraints in a single cluster, the projected mass distribution of these clusters can be determined with unprecedented spatial resolution, and even very small subcomponents will be detectable. In addition, each strong lensing cluster will produce many highly magnified galaxy images, so that the already truly impressive light-collecting power of NGST can be coupled with these natural telescopes to map even fainter galaxies. The ‘transition zone’ between strong and weak lensing, in which hundreds of arclets will be found, can be used to obtain redshift estimates from the degree of their distortions, thus providing an independent means to measure the redshifts of the faintest galaxies observable with

NGST (see, e.g., Kneib et al 1994; Ebbels et al. 1996, 1998).

The detailed mass models of clusters over a broad range of redshifts, and its comparison with other observables (such as X-ray emission, SZ-depletion, and galaxy distribution) will permit a thorough study of the relation between the dark and the baryonic matter in clusters. Questions like the validity of hydrostatic equilibrium of intra-cluster gas, the gas-to-mass fraction as a function of cluster mass and redshift, the possible presence of non-thermal pressure etc. can be investigated in great detail.

Cluster with such a large number of strong lensing features also provide a direct and purely geometrical handle on cosmological parameters, again through the dependence of the lensing strength on D_{ds}/D_s (e.g., Link & Pierce 1998). Whereas this method could in principle also be applied to current observations of multiple strong lensing features in cluster, most of the strong lensing features are too faint to obtain a reliable redshift, and in addition, one can also trade details of the mass distribution for changes in D_{ds}/D_s . This will not be the case if the number of strong lensing features becomes much larger.

6. MEASURING THE STATISTICAL PROPERTIES OF THE DARK MATTER DISTRIBUTION IN THE UNIVERSE

The statistical properties of the distortion field of the images of high-redshift galaxies directly reflects the statistical properties of the intervening mass distribution. For example, the two-point ellipticity statistics (such as rms inside circular apertures, or correlation functions) depend directly on the appropriately weighted and projected power spectrum of the cosmic mass distribution (Blandford et al 1991; Kaiser 1992, 1998; Jain & Seljak 1997; Schneider et al 1998b; Seljak 1997). A preliminary detection of cosmic shear has been reported (Fort et al 1996; Schneider et al 1998a; Seitz 1998).

Cosmic shear is, besides CMB measurements, the cleanest probe of the LSS, since it makes no assumption on the relation between mass and light. Whereas the CMB can probe the LSS on comoving scales above about 10 Mpc, cosmic shear is sensitive also to much smaller scales; in particular, it can probe the non-linear evolution of the power spectrum. A comparison with the linear power spectrum then yields strong constraints on the evolution of the mass distribution, e.g., that of the power spectrum, at relatively late epochs. The gravitational instability picture of structure formation can therefore be tested with high accuracy. In addition, deep ‘blank-field’ imaging will also be used to define mass-selected samples of cluster, and in particular might find group- and/or cluster-mass halos which are very underluminous and therefore missed in standard cluster searches (‘dark clusters’). Such isolated halos form the highly non-Gaussian tail of the LSS, which provides invaluable information for the distinction between different cosmological model which may have the same projected linear power spectrum, or the same two-point statistics (e.g., Jain et al. 1998).

Ongoing and planned ground-based deep wide-field imaging surveys will measure the power spectrum and the halo abundance for typical redshifts of about 0.5; with NGST, this can be extended to redshifts of order 2 or

3 which requires a much higher number density of background galaxies and a considerably higher mean redshift for them. By comparing the projected dark matter distribution, statistically sliced into redshift bins according to the (magnitude-dependent) redshift distribution of the background galaxies (Seljak 1998), with the galaxy distribution at $z \lesssim 3$, the redshift- and scale dependence of the bias ‘factor’ can be studied in great detail (Schneider 1998; van Waerbeke 1998). For example, to obtain a statistically significant sample of ~ 1000 halos detected from their mass properties only, a total area of $\sim 10\text{deg}^2$ mapped down to $K \sim 27$ would be sufficient. This estimate depends strongly on the cosmological model (Kruse & Schneider 1998), and a conservative number – which applies to an EdS Universe – has been quoted. For an open model, the expected number of halos is about 3 times larger. As mentioned before, for such high redshifts the ‘dark halo confusion limit’ is reached (cf. the simulated shear maps by Jain et al 1998), so photometric redshift information of the *background* galaxies is essential to distinguish the tidal gravitational field of several mass concentrations along the same line-of-sight, using the redshift dependence of the lens effect.

Such a wide-field survey with NGST would also allow to directly search for arcs. As was pointed out by Bartelmann et al (1998), the statistics of arcs provides a very powerful handle on the cosmological parameters, with expectations differing by a factor ~ 100 between an EdS and an open Universe. They have shown that from the already known number of arcs, a cluster-normalized EdS model is highly disfavoured. This argument could be very much strengthened if a ‘field survey’ for arcs is undertaken. Since the majority of observed arcs are very thin, partly unresolved even with WFPC-2, the angular resolution provided by NGST will be invaluable for this search.

A first taste for the power of NGST to measure cosmic shear can be obtained from the STIS instrument onboard HST: in a 20 minute exposure taken with the CLEAR ‘filter’, a galaxy number density of $50 - 100 \text{ arcmin}^{-2}$ can be achieved; part of an ongoing parallel observing program will be used to measure cosmic shear on the (small) scale of STIS, 51 arcseconds, and first results have been reported by Seitz (1998). But NGST, with its much larger FOV and collecting area, and smaller pixel size will be tremendously more powerful.

7. DISCUSSION

The previous examples should have illustrated the power of NGST for weak lensing, i.e., to map the dark matter distribution at high redshifts. The discussion here has been at most semi-quantitative, for at least two reasons: First, NGST will probe the galaxy distribution at luminosities and redshifts that are fully unexplored up to now. Therefore, the statistical properties of the galaxy population seen by NGST (number density, redshift distribution, size distribution, etc.) can be estimated only very roughly. Second, weak lensing with NGST enters a regime which has not been considered seriously up to now, even by daring theoreticians. Most problematic is the crowding along the lines-of-sight to redshifts $z_s \sim 5$, mentioned before, and new statistical and theoretical tools need to be developed and tested with numerical simulations. However, by basing the discussion on the S/N estimate (2), the qualitative estimates presented here should closely approximate the true power of NGST for weak

lensing. Furthermore, our estimates were based on the assumption that K-band images will be used for weak lensing – this is not at all obvious. Certainly going to the NIR has the advantage of probing the rest-frame optical wavelengths, but it may be that a somewhat longer wavelength will turn out to be more efficient – but in the L or M band, even less is known about the galaxy population.

It should be stressed here that predictions for weak lensing applications with NGST are extremely daring, and that the present discussion provides a severe underestimate of these possibilities. To wit, assume 10 years ago someone would have been asked to predict the lensing applications of HST, or the VLT. At that time, arcs have just been discovered, and Fort et al (1988) published the first arclets. But none of the applications discussed above have been seriously mentioned in the literature, with the first weak lensing observation published in 1990 (Tyson et al 1990). In fact, only ten years ago the dense population of background galaxies was pointed out clearly by Tyson (1988). Given the strong rate of evolution in this field, it is easy to predict that the range of weak lensing applications of NGST are currently nearly unpredictable, in the sense that they are likely to be much broader than what was presented here.

ACKNOWLEDGEMENTS

We would like to thank Y. Mellier, R. Pello and S. Seitz for numerous discussions. This work was supported by the ‘‘Sonderforschungsbereich 375-95 f ur Astro-Teilchenphysik’’ der Deutschen Forschungsgemeinschaft and the TMR Network ‘‘Gravitational Lensing: New Constraints on Cosmology and the Distribution of Dark Matter’’ of the EC under contract No. ERBFMRX-CT97-0172. PS would like to thank the Observatoire de Midi-Pyr enes where most of this work has been done for its hospitality and support.

REFERENCES

- Bartelmann, M., Huss, A., Colberg, J.M., Jenkins, A. & Pearce, F.R. 1998, MNRAS, in press (also astro-ph/9709229).
- Bartelmann, M. & Narayan, R. 1995, ApJ 451, 60.
- Blandford, R.D., Saust, A.B., Brainerd, T.G. & Villumsen, J.V. 1991, MNRAS 251, 600.
- Bonnet, H. & Mellier, Y. 1995, A&A 303, 331.
- Bonnet, H., Mellier, Y. & Fort, B. 1994, ApJ 427, L83.
- Brainerd, T.G., Blandford, R.D. & Smail, I. 1996 ApJ 466, 623.
- Bruzual, G. & Charlos, S. 1993, ApJ 405, 538.
- Clowe, D., Luppino, G.A., Kaiser, N., Henry, J.P. & Gioia, I. 1998, ApJ 497, L61.
- Dalcanton, J., Spergel, D.N., Gunn, J.E., Schmidt, M. & Schneider, D.P. 1998, AJ 114, 2178.
- Dell’Antonio, I. & Tyson, J.A. 1996, ApJ 473, L17.
- Ebbels, T.M.D. et al. 1996, MNRAS 281, L75.
- Ebbels, T.M.D. et al. 1998, MNRAS 295, 75.
- Fahlman, G., Kaiser, N., Squires, G. & Woods, D. 1994, ApJ 437, 56.
- Fort, B., Prieur, J.L., Mathez, G., Mellier, Y. & Soucaill, G. 1988, A&A 200, L17.
- Fort, B., Mellier, Y., Dantel-Fort, M., Bonnet, H. & Kneib, J.-P. 1996, A&A, 310, 705.
- Geiger, B. & Schneider, P. 1998a, MNRAS 295, 497.
- Geiger, B. & Schneider, P. 1998b, MNRAS, submitted.
- Griffiths, R.E., Casertano, S., Im, M. & Ratnatunga, K.U. 1996, MNRAS 282, 1159.
- Hoekstra, H., Franx, M., Kuijken, K. & Squires, G. 1998, ApJ in press, also astro-ph/9711096.
- Hogg, D.W., Blandford, R.D., Kundic, T., Fassnacht, C.D. & Malhotra, S. 1996, ApJ 467, L73.
- Hudson, M.J., Gwyn, S.D.J., Dahle, H. & Kaiser, N. 1998, ApJ, in press, also astro-ph/9711341.
- Jain, B. & Seljak, U. 1997, ApJ 484, 560.
- Jain, B., Seljak, U. & White, S.D.M. 1998, astro-ph/9804238.
- Kaiser, N. 1992, ApJ 388, 272.
- Kaiser, N. 1998, ApJ 498, 26.
- Kaiser, N. & Squires, G. 1993, ApJ 404, 441.
- Kaiser, N., Squires, G. & Broadhurst, T. 1995, ApJ 449, 460.
- Kneib, J.-P., Mellier, Y., Fort, B. & Mathez, G. 1993, A&A 273, 370.
- Kneib, J.-P., Mathez, G., Fort, B., Mellier, Y., Soucaill, G. & Longaretti, P.-Y. 1994, A&A 286, 701.
- Kneib, J.-P. et al. 1995, A&A 303, 27.
- Kneib, J.-P., Ellis, R.S., Smail, I., Couch, W.J. & Sharples, R.M. 1996, ApJ 471, 643.
- Link, R. & Pierce, M.J. 1998, astro-ph/9802207.
- Luppino, G. & Kaiser, N. 1997a, ApJ 475, 20.
- Luppino, G. & Kaiser, N. 1997b, talk given at the ‘‘Workshop on Weak and cluster gravitational lensing’’, Ringberg Castle, Jan. 1997.
- Miralda-Escud , J. 1991, ApJ 380, 1.
- Natarajan, P. & Kneib, J.-P. 1997, MNRAS 287, 833.
- Natarajan, P., Kneib, J.-P., Smail, I. & Ellis, R.S. 1998, ApJ 499, 600.
- Olsen, L.F. et al. 1998, astro-ph/9803338.
- Postman, M. et al. 1996, AJ 111, 615.
- Schneider, P. 1996, MNRAS, 283, 837.
- Schneider, P. 1998, ApJ 498, 43.
- Schneider, P., Ehlers, J. & Falco, E.E. 1992, *Gravitational lenses*, Springer: New York.
- Schneider, P. & Rix, H.-W. 1997, ApJ 474, 25.
- Schneider, P., van Waerbeke, L., Mellier, Y., Jain, B., Seitz, S. & Fort, B. 1998a, A&A 333, 767.
- Schneider, P., van Waerbeke, L., Jain, B. & Kruse, G. 1998b, MNRAS 296, 873.
- Seitz, S. 1998, talk given at the IAP Meeting May 1998, Paris.
- Seitz, C., Kneib, J.-P., Schneider, P. & Seitz, S. 1996, A&A 314, 707.
- Seitz, S., Saglia, R.P., Bender, R., Hopp, U., Belloni, P. & Ziegler, B. 1998, MNRAS, in press (also astro-ph/9706023).
- Seitz, C. & Schneider, P. 1995, A&A 297, 287.

- Seitz, S. & Schneider, P. 1996, *A&A* 305, 383.
- Seitz, S., Schneider, P. & Bartelmann, M. 1998, *A&A* submitted, aslo astro-ph/9803038.
- Seljak, U. 1997, astro-ph/9711124
- Smail, I., Ellis, R.S., Fitchett, M.J. & Edge, A.C. 1995, *MNRAS* 273, 277.
- Squires, G. et al. 1996a, *ApJ* 461, 572.
- Squires, G., Kaiser, N., Fahlman, G., Babul, A. & Woods, D. 1996b, *ApJ* 469, 73.
- Tyson, J.A. 1988, *AJ* 96, 1.
- Tyson, J.A., Valdes, F. & Wenk, R.A. 1990, *ApJ* 349, L1.
- Van Waerbeke, L. 1998, *A&A*, in press (also astro-ph/9710244).
- Van Waerbeke, L., Mellier, Y., Schneider, P., Fort, B. & Mathez, G. 1997, *A&A* 317, 303.
- Wambsganss, J., Cen, R. & Ostriker, J.P. 1998, *ApJ* 494, 29.

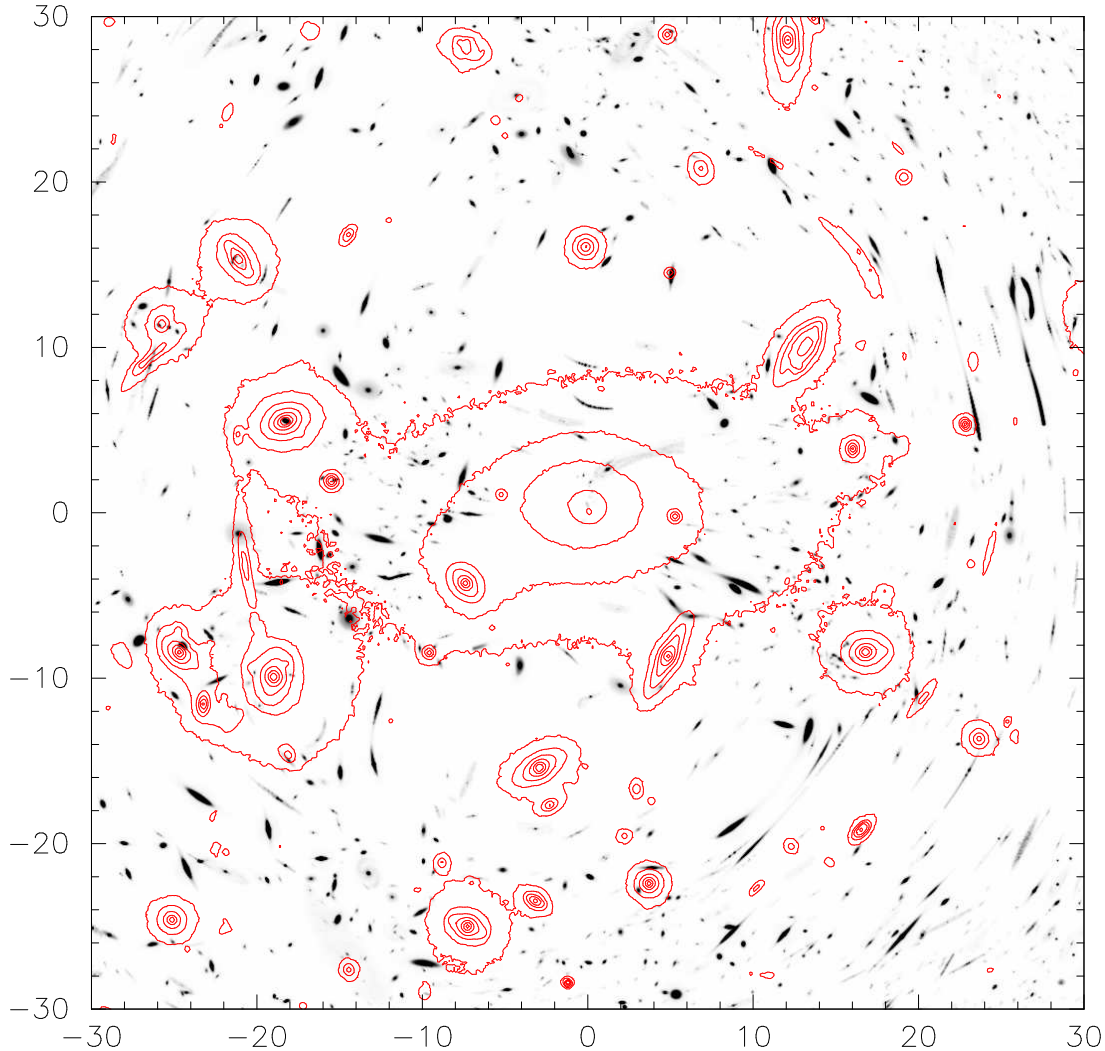


Figure 1. Simulated image of lensed features in the very central part of the massive cluster A2218. For these simulations, the mass profile of the cluster as constrained from HST observations and detailed modelling (Kneib et al 1996) has been used. The galaxy population model used in this simulation is somewhat simple (and likely to be highly oversimplified at such faint magnitudes). The number density of (unlensed) sources was assumed to be $4 \times 10^6 \text{deg}^{-2}$ down to $K=29$. To determine the physical quantities like absolute magnitude and intrinsic size, we applied the $K+e$ correction from Bruzual and Charlot (1993) galaxy synthesis model. To match current observations, we also include a size-dependence with redshift. The redshift distribution assumed is broad and extend to redshift $z \sim 10$ with a median value $z_{\text{med}} \sim 3$. The brighter objects (cluster galaxies and brightest arcs) seen by HST are displayed as contours, to make the faint galaxy images visible on this limited dynamic range reproduction. An enormous number of large arcs and arcslets are seen; in particular, numerous radial arcs can be easily detected, which will allow to determine the ‘core size’ of the cluster mass distribution. Due to the broad redshift distribution of the faint galaxies, arcs occur at quite a range of angular separations from the cluster center; this effect will become even stronger for higher-redshift clusters. It should be noted that this 1 arcminute field does not cover the second mass clump seen with HST; an NGST image will cover a much larger area, and more strong lensing features will be found which can then be combined with the weak lensing analysis of such a cluster. For this simulation we have used a 0.06 arcsecond pixel size; the NGST sampling will be better by a factor of 2.